Glucose depletion inhibits translation initiation via eIF4A loss and subsequent 48S preinitiation complex accumulation, while the pentose phosphate pathway is coordinately up-regulated

Lydia M. Castelli[a], Jennifer Lui[a], Susan G. Campbell[a,b], William Rowe[a], Leo A. H. Zeef[a], Leah E. A. Holmes[a], Nathaniel P. Hoyle[a,c], Jonathon Bone[a,d], Julian N. Selley[a], Paul F. G. Sims[e], and Mark P. Ashe[a]

[a]Faculty of Life Sciences, University of Manchester, Manchester M13 9PT, UK; [b]Biosciences Department, Faculty of Health and Wellbeing, Sheffield Hallam University, Sheffield S1 1WB, UK; [c]Developmental Genetics Laboratory, London Research Institute, Cancer Research UK, London WC2A 4LY, UK; [d]CoMPLEX, University College London, London WC1E 6BT, UK; [e]Faculty of Life Sciences, Manchester Interdisciplinary Biocentre, University of Manchester, Manchester M1 7DN, UK

ABSTRACT **Cellular stress can globally inhibit translation initiation, and glucose removal from yeast causes one of the most dramatic effects in terms of rapidity and scale. Here we show that the same rapid inhibition occurs during yeast growth as glucose levels diminish. We characterize this novel regulation showing that it involves alterations within the 48S preinitiation complex. In particular, the interaction between eIF4A and eIF4G is destabilized, leading to a temporary stabilization of the eIF3–eIF4G interaction on the 48S complex. Under such conditions, specific mRNAs that are important for the adaptation to the new conditions must continue to be translated. We have determined which mRNAs remain translated early after glucose starvation. These experiments enable us to provide a physiological context for this translational regulation by ascribing defined functions that are translationally maintained or up-regulated. Overrepresented in this class of mRNA are those involved in carbohydrate metabolism, including several mRNAs from the pentose phosphate pathway. Our data support a hypothesis that a concerted preemptive activation of the pentose phosphate pathway, which targets both mRNA transcription and translation, is important for the transition from fermentative to respiratory growth in yeast.**

Monitoring Editor
Thomas D. Fox
Cornell University

Received: Feb 23, 2011
Revised: Jun 15, 2011
Accepted: Jul 20, 2011

INTRODUCTION

The bulk biosynthesis of proteins represents one of the most energy-demanding activities in cells. For instance, recent estimates suggest that as many as 13,000 proteins are produced per second in each actively growing yeast cell (von der Haar, 2008). This rate balances protein degradation and allows for high rates of cell division. On the basis of this alone, it is apparent that, in response to stress conditions, cells would need to dramatically attenuate protein synthesis to maintain energy reserves and instigate a stress-specific gene expression program. Indeed, a variety of cellular stresses have been shown to rapidly induce a global inhibition of protein synthesis at the level of translation initiation (Holmes *et al.*, 2004; Spriggs *et al.*, 2010).

Eukaryotic translation initiation is an intricate process involving many multisubunit protein and ribonucleoprotein complexes (Jackson *et al.*, 2010). For instance, a closed-loop complex forms on the mRNA (Wells *et al.*, 1998). In this complex eIF4E interacts with the 5′ mRNA cap structure along with a molecular scaffold protein,

This article was published online ahead of print in MBoC in Press (http://www.molbiolcell.org/cgi/doi/10.1091/mbc.E11-02-0153) on July 27, 2011.

Address correspondence to: Mark P. Ashe (Mark.P.Ashe@manchester.ac.uk).

Abbreviations used: 4E-BP, eIF4E binding protein; DEPC, diethylpyrocarbonate; DTT, dithiothreitol; GDP, guanosine diphosphate; GTP, guanosine-5′-triphosphate; HRP, horseradish peroxidase; IgG, immunoglobulin G; NADPH, reduced NADP; NP-40, Nonidet P-40; qRT-PCR, quantitative real-time reverse transcriptase PCR analysis; SC, synthetic complete; TAP, tandem affinity purification; uORF, upstream open reading frame; UTR, untranslated region; YP, yeast extract/peptone.

© 2011 Castelli *et al.* This article is distributed by The American Society for Cell Biology under license from the author(s). Two months after publication it is available to the public under an Attribution–Noncommercial–Share Alike 3.0 Unported Creative Commons License (http://creativecommons.org/licenses/by-nc-sa/3.0).

"ASCB®," "The American Society for Cell Biology®," and "Molecular Biology of the Cell®" are registered trademarks of The American Society of Cell Biology.

eIF4G, and the eIF4A ATP-dependent RNA helicase: Pab1p interacts both with the mRNA 3′ poly(A) tail and with eIF4G. In addition, a 43S complex forms via the interaction of a host of translation initiation factors with the small ribosomal (40S) subunit (Pestova *et al.*, 2007). One such factor, eIF2, when bound to guanosine-5′-triphosphate (GTP), recruits the initiator methionyl-tRNA to form the ternary complex (eIF2.GTP Met-tRNA^{i}), which interacts with the 40S ribosomal subunit.

The selection of an mRNA from a competitive pool for translation relies on the interaction of the closed loop mRNP complex with the 43S complex to form the 48S preinitiation complex. Formation of the 48S complex requires protein–protein interactions between components of the closed loop and 43S complexes. In mammalian cells, eIF4G in the closed loop complex interacts with the e subunit of eIF3 on the 43S complex (LeFebvre *et al.*, 2006). In yeast, however, an interaction between eIF3 and eIF4G has not been observed, and interactions between eIF4G and other components of the 43S complex, such as eIF1 and eIF5, are thought to promote 48S complex formation (He *et al.*, 2003). Following formation of the 48S complex, a linear scanning process occurs that culminates in the recognition of the first downstream mRNA start codon. Upon start codon recognition, the GTP on eIF2 becomes hydrolyzed to guanosine diphosphate (GDP). This hydrolysis promotes global conformational changes and the loss of many translation initiation factors allowing the joining of the 60S ribosomal subunit (Jackson *et al.*, 2010). After translation initiation, eIF2 is left in a GDP-bound form. eIF2B is a heteropentameric guanine nucleotide exchange factor that is responsible for recycling eIF2 from a GDP-bound form back to the GTP-bound form. Therefore, eIF2B replenishes the translationally active form of eIF2 to directly facilitate the formation of ternary complex (Pavitt, 2005).

Highly conserved mechanisms allow eukaryotic cells to globally reduce the level of protein synthesis (Jackson *et al.*, 2010). One of the more prominent examples involves eIF2α kinases (Wek *et al.*, 2006). Activation of these kinases in response to environmental or intracellular cues causes phosphorylation of the α subunit of the eukaryotic translation initiation factor eIF2. Phosphorylated eIF2 serves as an inhibitor of the eIF2B-mediated guanine nucleotide exchange reaction leading to reduced rates of translation initiation. Specific examples of mRNAs that are immune to this regulation have been characterized.

The established example of such an mRNA is *GCN4* in yeast which is activated under stress conditions, such as amino acid starvation (Hinnebusch, 2005). Such stress conditions activate the sole *Saccharomyces cerevisaie* eIF2α kinase, Gcn2p, to phosphorylate eIF2α, which reduces eIF2B activity leading to reduced ternary complex (eIF2.GTP Met-tRNA^{i}) levels. Under these stress conditions, *GCN4* mRNA is translationally activated by virtue of four upstream open reading frames (uORFs) and a complex reinitiation mechanism. Following translation of the first uORF in the *GCN4* mRNA, an unusual translation termination event occurs where, rather than dissociating, the translating ribosome resumes a form of ribosomal scanning. Before reinitiation can occur, however, the ribosome must reacquire the initiator methionyl-tRNA in the form of the ternary complex. Therefore, under nonstress conditions where ternary complex levels are high, the ribosome reacquires the ternary complex rapidly to reinitiate at one of the other three uORFs. More typical termination events, particularly at uORF4, then lead to ribosome dissociation. However, under stress conditions, ternary complex can be reacquired after the ribosome has passed the uORFs and hence translation of the *GCN4* ORF increases. The same basic mechanism is thought to activate the *ATF4* mRNA in mammalian cells in response to a variety of stresses (Wek *et al.*, 2006). Yeast *GCN4* mRNA translation can also be activated under conditions that regulate eIF2B activity in mechanisms that are independent of eIF2α phosphorylation. For instance, both fusel alcohols and volatile anesthetics cause up-regulation of *GCN4* translation by inhibiting eIF2B in *S. cerevisiae* (Ashe *et al.*, 2001; Palmer *et al.*, 2005).

Targeting of the mRNA closed loop complex is another conserved mechanism by which translation initiation is regulated at both global and mRNA-specific levels. For instance, a series of eIF4E binding proteins (4E-BPs) have been described that can compete with eIF4G in terms of eIF4E binding. These proteins can globally regulate protein synthesis in a manner that is responsive to alterations in phosphorylation status, as in the case of 4E-BP1, or they can be targeted to specific mRNAs via RNA binding protein interactions, as in the case of *Drosophila* Cup and *Xenopus* Maskin (Richter and Sonenberg, 2005). *S. cerevisiae* harbors two 4E-BPs, Caf20p and Eap1p, which appear to target different sets of mRNA to impact pseudohyphal growth (Ibrahimo *et al.*, 2006). Recently it has been proposed that differential binding to the various Puf proteins may explain some of the mRNA-specific effects of the *S. cerevisiae* 4E-BPs (Cridge *et al.*, 2010); however, global controls that rely on these 4E-BPs have also been described. For instance, Eap1p is involved in global mechanisms targeting translation initiation as a consequence of membrane or oxidative stress (Deloche *et al.*, 2004; Mascarenhas *et al.*, 2008).

Of the stresses studied that target translation initiation in the yeast *S. cerevisiae*, glucose depletion causes the most dramatic inhibitory effect, in terms of both rapidity and scale of the reduction in protein production (Holmes *et al.*, 2004). Glucose serves as a primary source of energy for most organisms, from bacteria to humans, and it is the favored carbon source for *S. cerevisiae*, as well as a variety of tissues/cell types in humans (e.g., brain, reticulocytes, and skeletal muscle). In yeast, as well as causing a global reduction in protein synthesis, glucose depletion leads to a derepression of the glucose repression pathway, which is a major system for controlling yeast carbohydrate metabolism. Indeed ~30% of yeast genes, which function in alternative carbohydrate metabolism and respiration, are transcriptionally repressed in glucose-replete conditions but become derepressed after glucose depletion (DeRisi *et al.*, 1997). The pathways controlling this global transcriptional switch are well-characterized (Rolland *et al.*, 2002), but do not appear to play a major role in the inhibition of protein synthesis (Ashe *et al.*, 2000; Lui *et al.*, 2010). Indeed, the shutdown of protein production is somewhat at odds with the transcriptional derepression. One possible rationale is that the reduction in protein synthesis serves as an interlude during which existing mRNAs/proteins are degraded, to facilitate a subsequent transcriptional switch in gene expression profile. Moreover, specialized mechanisms might exist to allow the translational maintenance of specific mRNAs that are required for adaptation to the stress.

In this study, we further characterize the stage of protein synthesis that is inhibited following glucose starvation. We provide evidence for loss of the eIF4A translation factor and stabilized protein–protein interactions within the 48S complex; this evidence points to translational inhibition at a step after 48S complex formation. We use microarray analyses to provide detailed quantitative and reproducible comparisons of the levels of cellular mRNAs and their translational status following glucose depletion. In particular, we focus on the regulation of the pentose phosphate pathway and the onset of respiration many hours after glucose depletion as important processes that may be regulated at the translational level.

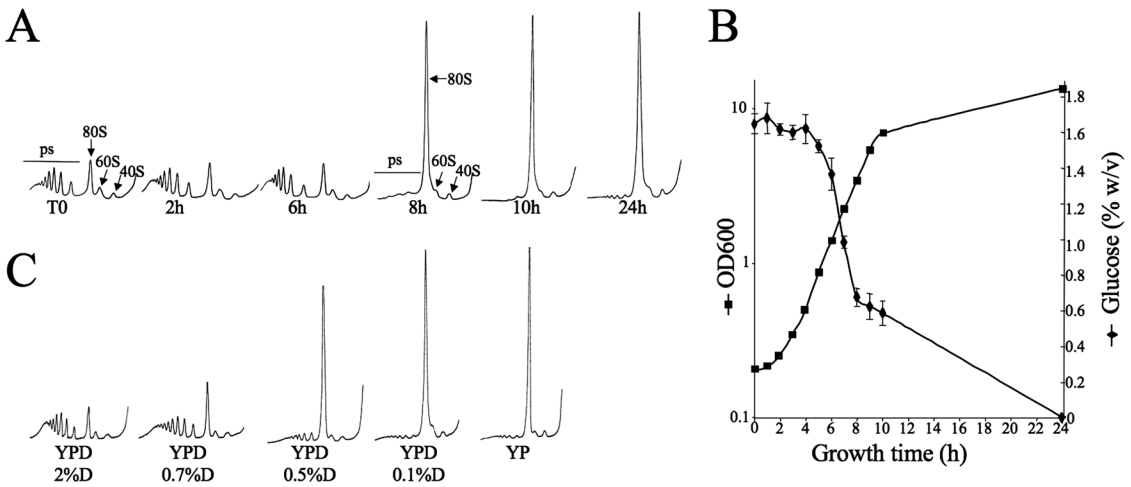

FIGURE 1: A defined decrease in glucose concentration causes translational inhibition. (A) Polysome traces from the growth analysis presented in B for the yMK36 strain grown in YPD and sampled at various time points. Polysomes were analyzed as described in *Materials and Methods*. The 40S (small ribosomal subunit), 60S (large ribosomal subunit), 80S (monosome), and polysome peaks are labeled. (B) Growth curve derived from three biological replicate cultures of *S. cerevisiae* over a 24-h period (OD_{600}), showing utilization of glucose in % (wt/vol). For these growth curves, three single colonies were each grown simultaneously under identical nutritional and growth conditions. (C) Polysome profiles from the yMK36 strain switched into media containing different glucose concentrations (2%, 0.7%, 0.5%, and 0.1% [wt/vol] glucose) for 10 min.

RESULTS

Translational inhibition at a defined point in the depletion of glucose during batch culture

Previously, we have observed the inhibition of translation initiation following the rapid depletion of glucose from yeast media (Ashe *et al.*, 2000; Holmes *et al.*, 2004). To ascertain whether a similar inhibition is observed following the gradual glucose exhaustion over the period of a batch culture, polysome analysis was performed at various stages of a culture's growth on rich glucose-containing media. As anticipated, the concentration of glucose in the media decreases with culture growth (Figure 1B). Polysome profiles indicative of highly active protein synthesis were observed when glucose levels decreased to 1% (wt/vol). Interestingly, when glucose levels decreased beyond 0.6% (wt/vol), an inhibition of translation initiation was observed as indicated by a decrease in polysome peaks and a subsequent increase in the 80S monosome peak (Figure 1A).

The impact of diminishing glucose levels below 0.6% (wt/vol) on translation initiation in batch culture might be a direct result of the decrease in glucose concentration, or it is plausible that increased cell density or the accumulation of waste products may play a role. To distinguish between these possibilities, yeast cells were grown to the mid-exponential phase and washed for 10 min in YP medium containing various concentrations of glucose (2.0, 0.7, 0.5, and 0.1% wt/vol). As shown in Figure 1C, the cells continued translating in the presence of 2.0 and 0.7% (wt/vol) glucose; however, translation became inhibited when cells were exposed to medium containing glucose levels of 0.5% (wt/vol) or lower. Therefore it appears there is a finite concentration of glucose that is required in a yeast batch culture to maintain protein synthesis and that this concentration is surprisingly high. This finding implies that protein synthesis is specifically attenuated at a stage in culture growth when there is still sufficient glucose available for another cycle of cell division, but it is likely that this will then be depleted. These results suggest that the inhibition of translation represents a preemptive conservation of cellular resources in preparation for the global shift in metabolism that occurs during diauxie.

Translational inhibition does not rely on eIF2B inhibition or 4E-BP activation

In previous studies, we have suggested that the inhibition of translation initiation caused by glucose starvation is the result of a novel regulatory mechanism (Ashe *et al.*, 2000; Holmes *et al.*, 2004). After extended periods of glucose starvation (several hours), however, activation of Gcn4p translation is observed (Yang *et al.*, 2000). In addition, more recently after 20–30 min of glucose depletion, a decrease in eIF2α phosphorylation has been observed (Cherkasova *et al.*, 2010). Finally, in higher cells, glucose regulates protein synthesis via effects on the level of phosphorylated eIF2α (Scheuner *et al.*, 2001; Gomez *et al.*, 2004). To investigate this possible mechanism in more detail with regard to the glucose-dependent translational regulation in yeast, we instigated a series of experiments to evaluate eIF2α phosphorylation and its consequences. Following glucose depletion, evidence of polysome run-off is first observable after 1 min, and after 5–10 min this run-off is complete (Ashe *et al.*, 2000). Therefore we investigated eIF2α phosphate levels 10 min after glucose starvation and compared this to other stress conditions (Figure 2A). Consistent with our previous results, we found that, in contrast to other stresses such as amino acid starvation and rapamycin treatment, glucose starvation does not rapidly induce increased levels of phosphorylated eIF2α. This finding agrees with those of genetic studies in which the inhibition of translation caused by glucose starvation was still evident in mutants of this pathway (Ashe *et al.*, 2000). After 20–30 min it is clear from our previous work, and that of others, that eIF2α is dephosphorylated (Hoyle *et al.*, 2007; Cherkasova *et al.*, 2010). This dephosphorylation may represent a consequence of the inhibition of translation or may be involved in translational reprogramming. Overall, these results show that glucose starvation does not bring about the global reduction in protein synthesis by regulating eIF2B activity in a manner that is dependent on changes in eIF2α phosphorylation.

We have also shown that eIF2B activity can be inhibited independently of eIF2α phosphorylation in response to fusel alcohols (Taylor *et al.*, 2010). A hallmark of eIF2B-dependent translation controls in yeast is the translational activation of the *GCN4* mRNA.

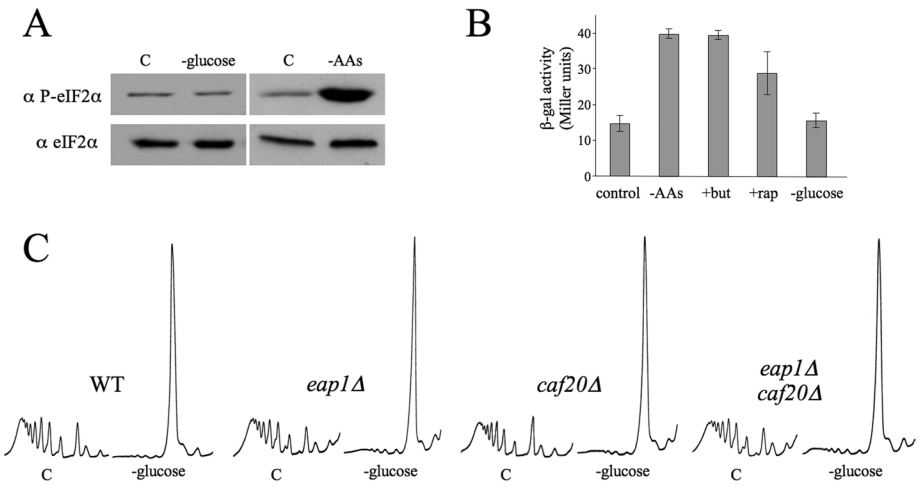

FIGURE 2: Inhibition of translation initiation following glucose starvation does not occur through previously identified mechanisms. (A) Western blots from the yMK36 strains following growth in SCD. Cells were pelleted and resuspended in complete media (C), media lacking amino acids (–Aas), or media lacking glucose (–glucose) for 10 min. The protein sample sets were loaded in duplicate and blotted, and the blots were split and probed separately with antibodies to eIF2α and phosphospecific antibodies to phosphoserine 51 on eIF2α. (B) β-Galactosidase assays measured in Miller units from extracts prepared from strain yMK926 (bearing a *GCN4-lacZ* reporter). Strains were grown in SCD medium, pelleted, then transferred for 1 h to complete SCD medium under a range of conditions: C (complete media), –AAs (media lacking amino acids), –glucose (media lacking glucose), +but (media with 1% [vol/vol] 1-butanol), and +rap (medium with 0.2 μg/ml rapamycin). Error bars represent the SD from three independent experiments. (C) Polysome profiles from the yMK1750 (BY4741-derived wild type), YMK1751 (*caf20*Δ), yMK1752 (*eap1*Δ), and yMK1752 (*caf20*Δ *eap1*Δ) strains. Strains were pelleted and switched into either complete medium or medium lacking glucose for 10 min.

A standard method to evaluate the translational regulation of *GCN4* is the use of an integrated *GCN4-lacZ* reporter in which the promoter and 5′ untranslated region (UTR) of *GCN4* have been fused to the gene for β-galactosidase (Dever, 1997). Using this approach, we discovered that, even though amino acid starvation, rapamycin treatment, and butanol addition all caused an increase in *GCN4* translation, glucose depletion led to little or no change (Figure 2B). Thus it seems highly unlikely that glucose depletion impacts translation initiation via effects at the level of eIF2B.

It has also been shown that the 4E-BPs can play a role in the regulation of translation initiation in yeast in response to specific forms of oxidative and membrane stress (Deloche *et al.*, 2004; Mascarenhas *et al.*, 2008). In addition, it is known that the PAS kinases, Psk1p and Psk2p, which have roles in the regulation of glucose utilization, can phosphorylate the yeast 4E-BP, Caf20p (Rutter *et al.*, 2002). To conclusively determine whether either of the yeast 4E-BPs plays a role in the translation inhibition elicited by glucose depletion, strains bearing deletions in the *CAF20* and *EAP1* genes were evaluated for alterations in the inhibitory response. Both the single and double mutant strains exhibited the same dramatic alteration in polysome profile that is observed in the wild-type strain (Figure 2C). Thus it is unlikely that either of the yeast 4E-BPs plays a role in this translation inhibition. Furthermore, we previously showed no difference in the levels of eIF4G that are associated with eIF4E, no difference in the capacity of eIF4E to bind to a cap affinity column, and no difference in the capacity of eIF4G and Pab1p to be purified on a poly(A) affinity column (Hoyle *et al.*, 2007). This finding suggests that the closed loop complex and the interactions required for its formation are not targeted as part of a response to glucose starvation.

Alterations within the 48S preinitiation complex following glucose starvation

To investigate individual factors and complexes in the initiation pathway during the glucose starvation response, we undertook a tandem affinity purification (TAP) strategy. As part of this work, we noticed some striking changes in translation factor copurifications within the 48S preinitiation complex that were dependent on glucose starvation. For example, following affinity purification of the eIF3 complex via the eIF3b subunit, we observed a substantial increase in the levels of eIF4G and Pab1p copurifying with eIF3 10 min after glucose starvation (Figure 3A, eIF3b-TAP). Similarly, the reciprocal eIF4G-TAP showed the same result with higher levels of copurifying eIF3 apparent after a 10-min glucose starvation (Figure 3A, eIF4G-TAP). This result was particularly surprising, because neither eIF4G or the other mRNA-binding translation initiation factors, eIF4E and Pab1p, immunopurify with eIF3 or vice versa (He *et al.*, 2003). In contrast, in the mammalian system, an eIF3e–eIF4G interaction is viewed as paramount to the recruitment of the 43S complex to mRNA (LeFebvre *et al.*, 2006). To confirm that an interaction between the closed loop complex and a component of the 43S complex is stabilized as part of the translation inhibition elicited by glucose starvation in yeast, we also tested copurification of eIF3 with Pab1p. As with the eIF4G purification, we observed greater levels of eIF3 interaction with Pab1p after glucose starvation (Figure 3A, Pab1p-TAP).

Previously, we have shown that eIF4E, eIF4G, and Pab1p in association with mRNA relocate to processing (P) bodies and other bodies termed "EGP-bodies" following glucose starvation (Hoyle *et al.*, 2007). The increased stabilization of eIF3 with eIF4G, eIF4E, and Pab1p described earlier in the text is potentially at odds with these observations, as the closed loop complex would not be free to relocate to these cytoplasmic bodies. Relocalization of the closed loop complex first occurs many minutes after glucose starvation, however (Hoyle *et al.*, 2007; Buchan *et al.*, 2008). On this basis we repeated the affinity purifications both at 10 and 30 min after glucose depletion. Intriguingly, the increased levels of eIF3 copurification with the closed loop complex that are observed at the 10-min time point are no longer observed 30 min after glucose starvation (Figure 3B). These observations suggest that glucose starvation causes a transient buildup of complexes containing eIF4E, eIF4G, Pab1p, and eIF3, yet at later times, this complex has decayed, leaving the closed loop complex free to relocalize to cytoplasmic granules. The simplest interpretation of these results is that a step downstream of 48S complex formation is inhibited, leading to a transient accumulation of the 48S complex.

An analysis of cosedimentation of translation initiation factors across sucrose gradients lends further support to this interpretation. After a 10-min glucose starvation, eIF4G and Pab1p accumulate in the 40S fraction along with eIF3 (Figure 3D). After longer periods of glucose starvation, however, in results consistent with those of our previous studies (Hoyle *et al.*, 2007), eIF4G and Pab1p are largely found separate from the 40S peak, with a substantial

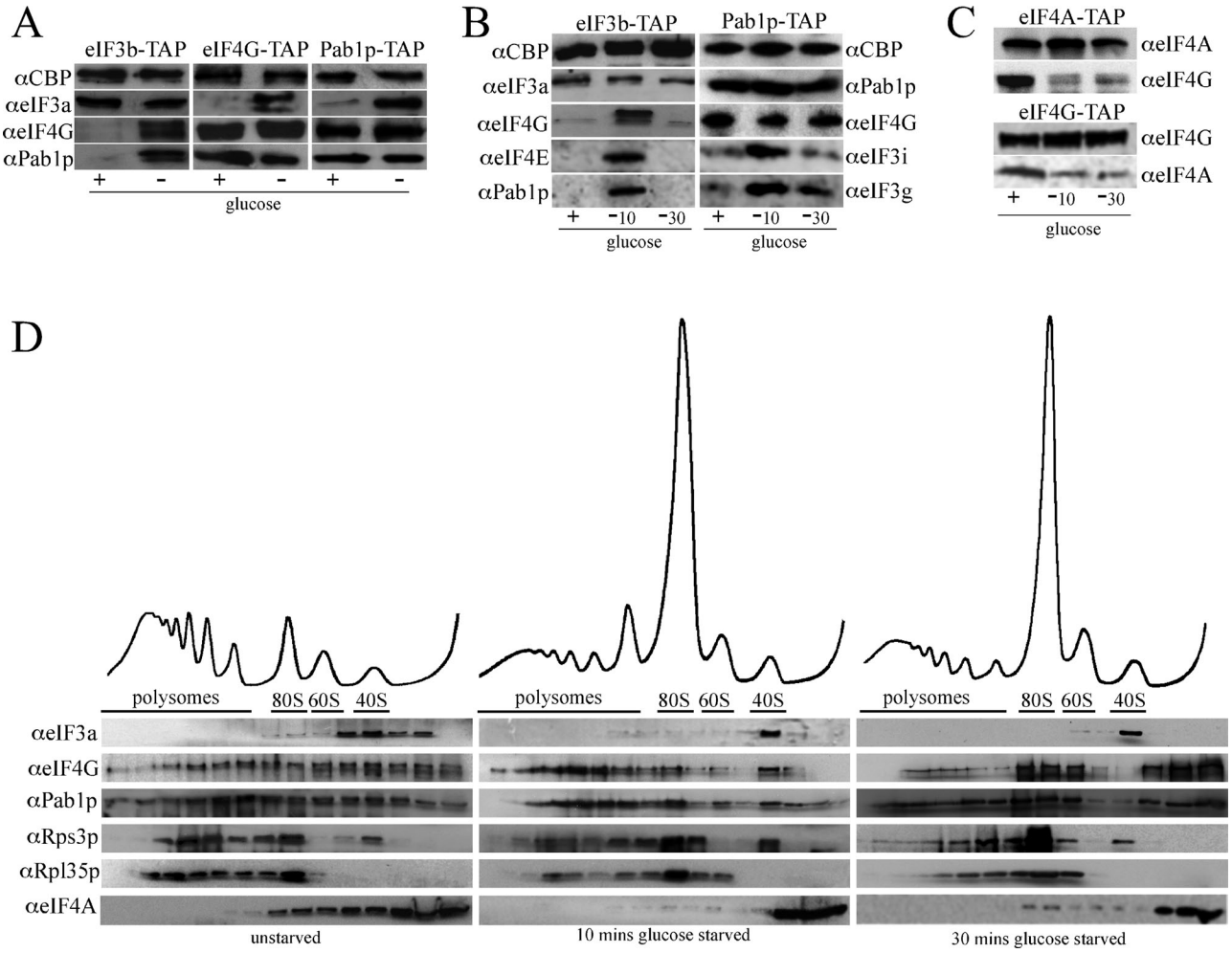

FIGURE 3: Investigation of translation initiation complexes suggests that a stalling of the initiation machinery results in the inhibition observed following glucose starvation. (A) Western blots on affinity purifications of complexes from whole-cell extracts prepared from cells that had been either glucose starved or unstarved of glucose for 10 min. The yMK1338 (*PRT1-TAP* [eIF3b]), yMK1316 (*TIF4631-TAP* [eIF4G1]), and yMK1342 (PAB1-TAP) strains were used, and the resulting Western blots were probed with αCBP (detects the calmodulin binding peptide part of the TAP tag), αeIF4G1, αeIF3a, αeIF4G, and αPab1p. The images presented derive from the same blot, as the blot was cut into slices, and each slice probed separately with the various different antibodies or reprobed. (B) As in A, except two different starvation time points were analyzed: 10 and 30 min for the strains yMK1338 (*PRT1-TAP* [eIF3b]) and yMK1342 (*PAB1-TAP*). α eIF3i and α eIF3g antibodies were used to detect eIF3. (C) As in B, except strains yMK1341 (*TIF1-TAP* [eIF4A]) and yMK1316 (*TIF4631-TAP* [eIF4G1]) were used, and the Western blots were probed with αeIF4A and αeIF4G1 antibodies. (D) Sucrose density gradient analysis of extracts from yeast grown in YPD and resuspended in either YPD (+glucose) or YP (-glucose) for 10 or 30 min then formaldehyde treated. Fractions were analyzed by SDS–PAGE and immunoblotting using antibodies raised against the proteins specified adjacent to each panel.

accumulation at the top of the gradient. Therefore it seems that the block in translation initiation causes a transient buildup of the 48S complex and the most likely inhibited steps that might result in this are the scanning or AUG recognition steps.

Glucose starvation destabilizes the eIF4A–eIF4G complex

In addition to changes at the level of eIF3 binding to eIF4G, we observed alterations to the amount of eIF4A bound to eIF4G. In this case, glucose starvation causes a clear reduction in the level of the eIF4G–eIF4A complex; a reduction that is sustained at both the 10- and 30-min time points (Figure 3C). This reduced association is further corroborated by studies on the level of cosedimentation of eIF4A with ribosome-containing fractions across a polysome gradient (Figure 3D). It seems likely that either the eIF4G or eIF4A subunits are posttranslationally modified to bring about this alteration; however, we have found little evidence for changes in the global phosphorylation status of these factors following glucose starvation (unpublished data). Overall, the buildup of the 48S complex and the reduced eIF4G–eIF4A interaction will likely play key roles in the mechanism of glucose-dependent translation regulation in yeast (see *Discussion* for more details). Other alterations to the translation machinery that have been observed as a result of glucose starvation, such as altered phosphorylation of various factors including eIF2α and Caf20p, may well play a role in sustained translation of particular mRNAs during the global shutdown.

Microarray analysis reveals a global change in gene expression following glucose starvation

Previously, we and others have identified mRNAs that exhibit sustained translation under stress conditions, using a polysomal

microarray strategy (Smirnova *et al.*, 2005; Shenton *et al.*, 2006; Melamed and Arava, 2007). Polysomal microarray analysis allows the study of global changes in protein synthesis. In brief, mRNAs are fractionated on the basis of how actively they are translated via polysome analysis, and these mRNA fractions are processed and applied to microarrays. In pioneering early studies, this approach was taken to investigate a switch in carbon source from glucose to glycerol/ethanol (Kuhn *et al.*, 2001). Relatively few mRNAs, however, were identified as differentially translated between the stressed and unstressed samples. Therefore, we extended this early analysis and made use of the greater quantitative range of more contemporary microarray systems to explore whether further mRNAs continue to be translated during the global shutdown observed during glucose starvation.

Cell extracts were made from exponential yeast cultures that were incubated for 10 min in media with or without glucose. These conditions led to the anticipated alteration in polysome profile with the starved culture exhibiting profound polysomal run-off (Figure 4A). From triplicate experiments individual monosomal or polysomal fractions were prepared, as described previously (Smirnova *et al.*, 2005). RNA was extracted from these fractions and, along with total RNA samples, each sample/fraction was processed into cRNA and subsequently hybridized to the Yeast Genome 2.0 array. Standard MA plots (allowing the comparison of individual microarray data sets) (Supplemental Figures 1–3) and statistical analysis of variance tests (unpublished data) indicated that there was only modest dispersal between biological replicate samples, confirming that the arrays are highly reliable reporters of relative transcript abundance in our samples. As anticipated, a tight cluster of data points was observed when biological replicate preparations of the total, polysome, or monosome fractions were compared. In contrast, comparison between the total, monosomal, and polysomal RNA samples reveals a broader spread of data points (Supplemental Figures 1–3).

Data were processed as described in *Materials and Methods* to generate two parameters, the change in transcript level and the change in translation state. A data set was accrued with mRNAs that are significantly up- or down-regulated at the transcript level and/or the translation level following glucose starvation. At the transcript level a total of 774 mRNAs were altered, >2-fold (444 up and 317 down). A total of 1005 mRNAs significantly changed translationally following glucose starvation, >1.9-fold (256 up and 749 down). To provide a more robust statistical set of regulated genes, significance analysis of microarrays ($p < 0.001$ and $q < 0.05$) was applied to the data. By definition, this analysis will significant reduce the level of false positives within the data set providing a core of regulated genes for further bioinformatics analysis. It is important to note, however, that the application of this false discovery rate via the *q* value cut-off will mean that regulated transcripts may well have been omitted at this point. This regulated data set amounts to a total of 688 mRNAs that were significantly altered, >2-fold (390 up and 298 down) at the transcript level, and a total of 226 mRNAs that are significantly changed translationally following glucose starvation, >1.9-fold (81 up and 145 down).

In response to stresses such as amino acid starvation, rapamycin treatment, and heat shock, a specific subset of genes is coregulated at both the transcriptional and translational level. This concept has been termed "potentiation" (Preiss *et al.*, 2003; Smirnova *et al.*, 2005), and there is some evidence for a similar phenomenon within this data set. For instance, after application of the q value cut-off, 54 mRNAs are coregulated at both the translational and transcript level (39 up and 15 down). In contrast, there is just a single example of an mRNA that increases transcriptionally, yet translation decreases and two mRNAs increase translationally while decreasing in terms of transcript levels. A full list of the mRNAs with altered profiles after the *q* value cut-off has been applied is shown in Supplemental Tables S2 and S3.

Classification and cluster analysis of mRNAs regulated following glucose starvation

To further dissect the physiological consequence of glucose starvation on yeast, the GOslim mapper (*Saccharomyces* Genome Database) and annotations on the Yeast Proteome Database were used to provide functional classifications of the translationally altered mRNAs (Supplemental Tables S2 and S3). This analysis revealed that many of the mRNAs that were translationally maintained following glucose starvation were involved in carbohydrate metabolism. Nitrogen, amino acid, nucleotide and alcohol metabolism and the general response to stress were also prominent functions, indicating an overall adaptation toward the exploitation of alternative carbon sources. The major classifications of the down-regulated mRNAs included cell cycle, cell transport, ribosome biogenesis, and transcription consistent with the general inhibition of growth and proliferation caused by glucose starvation. When the up-regulated and down-regulated data sets were subjected to over-/underrepresentation analysis, carbohydrate metabolism was notably overrepresented in the up-regulated data set, whereas translation was prominently underrepresented (Figure 4C).

The mRNAs with significantly altered translational profiles were separated into eight clusters based on the similarity of their transcript profiles using k-means and hierarchical clustering algorithms (Figure 4D). The data for each cluster are represented as a profile of the *z*-transformed (for each probe set, the mean is set to 0 and the SD to 1), in an Eisen color plot. Of these eight clusters, three contained mRNAs that were translationally maintained, and five contained those that were translationally down-regulated (Figure 4D). Ten of the 81 translationally up-regulated mRNAs fell within cluster 1, which showed that the increased monosome-to-polysome ratio observed was the result of a low expression of the mRNAs within the monosomal fractions following glucose withdrawal (Figure 4D). This finding suggests that the increase in translation state for these mRNAs may be the result of alterations in mRNA levels in the untranslated pool rather than increased translation following glucose starvation, and highlights the value of the comprehensive overview that clustering approaches provide. The vast majority of the translationally up-regulated mRNAs, however, fell within clusters 2 and 3, showing a profile in which a high expression of the mRNAs within the polysomal fractions is observed following glucose withdrawal (Figure 4D, expanded area). This pattern is consistent with a movement of these mRNAs into polysomes following glucose starvation, against the global trend of translation down-regulation.

Continued translation of specific mRNAs following glucose starvation

A subset of the mRNAs that showed altered profiles on the microarrays either at the transcript level or in their abundance across polysomal gradients were investigated using quantitative real-time reverse transcriptase PCR analysis (qRT-PCR). *ACT1* mRNA, which was not significantly altered in the array data sets, was used as a control to normalize the altered mRNAs. *HXT2*, *HSP30,* and *MTH1* exhibited increased transcript levels following glucose starvation, whereas the *AQR1*, *CDC6*, *PCL1,* and *RPA12* transcript levels decreased as measured by both qRT-PCR and microarray (Figure 5A). A similar correlation between the polysome microarray and the qRT-PCR

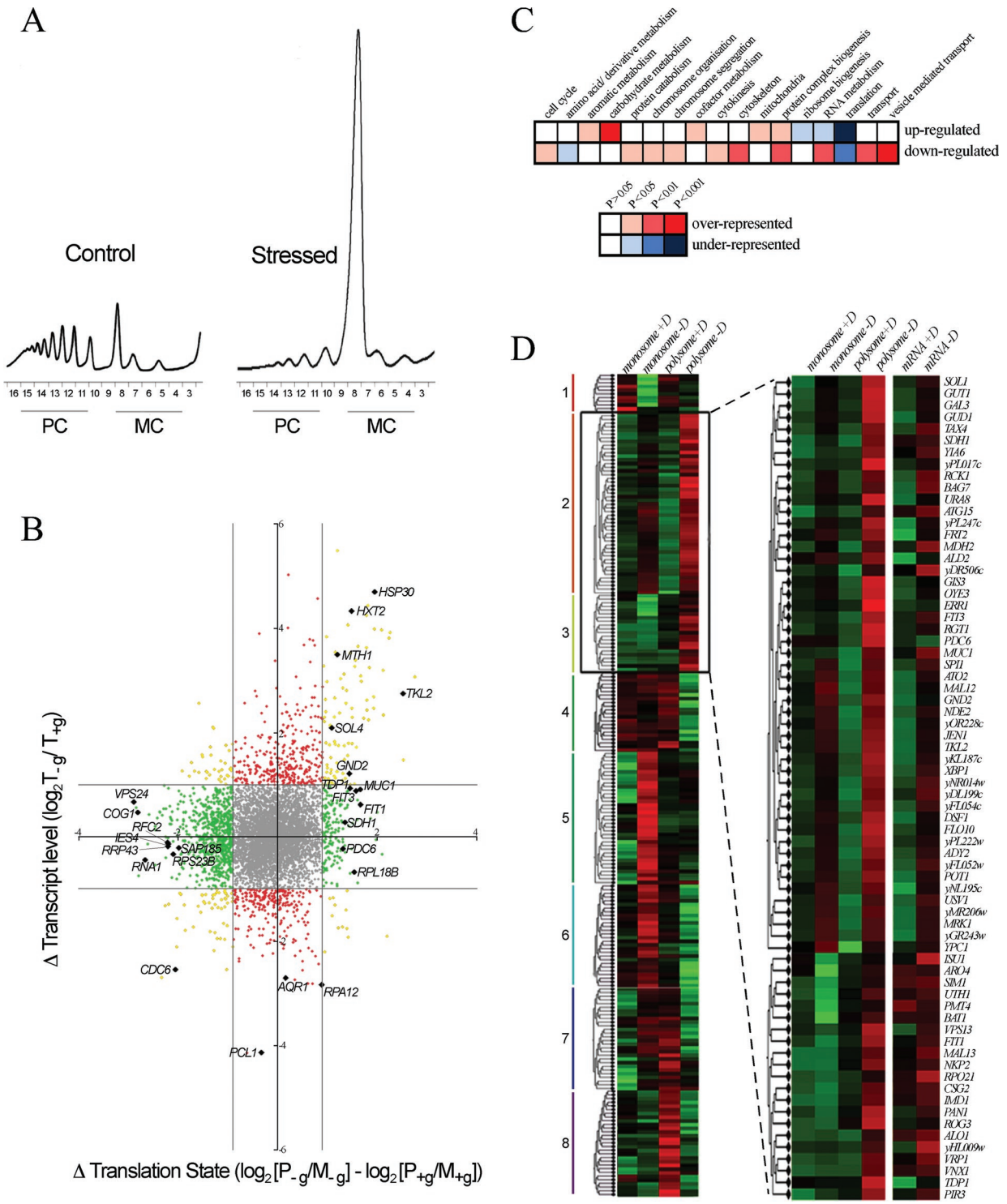

FIGURE 4: Polysomal microarray analysis shows global changes at both the transcript and translation level following glucose starvation. (A) Polysome profiles of control and glucose-starved yMK36 cultures, where the monosome (MC or MS) and polysome fractions (PC or PS) that were used for the arrays are highlighted. (B) Figure shows a graphical plot comparing transcript level (log_2[TS/TC]) with the change in translation state (log_2[PS/MS]- log_2[PC/MC]) after glucose depletion. Cutoff values of 1.0 and 0.9 for the change in transcript level and translation state, respectively, are depicted as dashed lines. Translationally regulated mRNAs that are not transcriptionally regulated are green, whereas mRNAs that are regulated solely at the transcript level are red. Translationally regulated mRNAs that are also regulated at the transcript level are yellow. Specific mRNAs that are relevant to subsequent experiments are labeled. (C) Over/underrepresentation analysis of the translational up- and down-regulated data sets. Carbohydrate metabolism is overrepresented, and translation is underrepresented in the translationally up-regulated data set. (D) Cluster analysis of the up- and down-regulated data sets with three clusters of up-regulated genes and five clusters of down-regulated genes. Clusters 2 and 3, which most likely represent mRNAs where translation is maintained or activated following glucose starvation, are expanded.

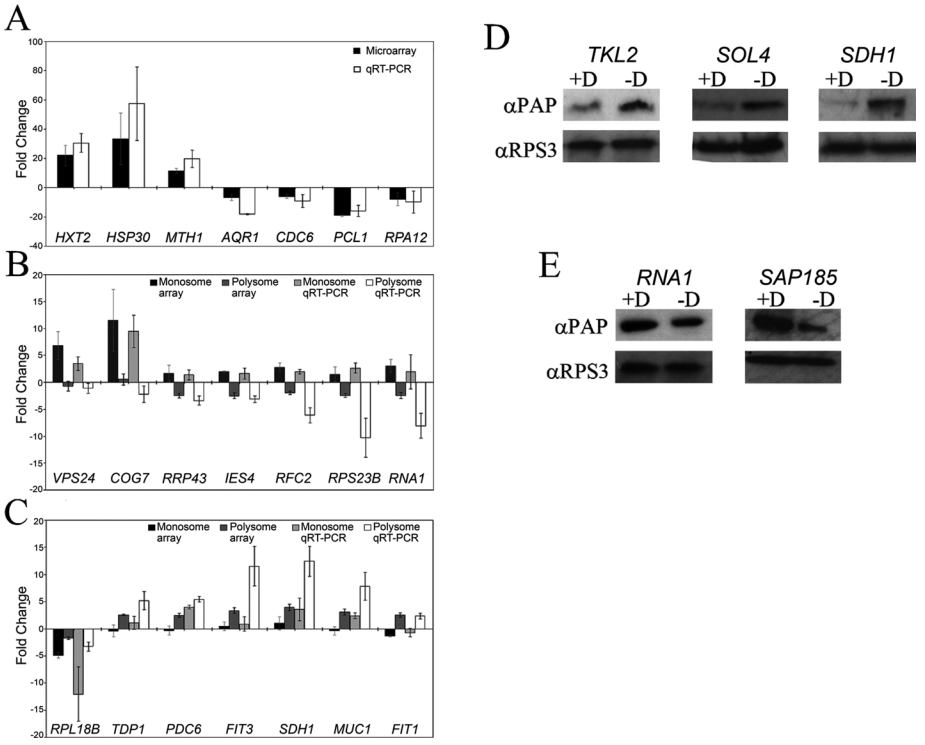

FIGURE 5: Validation of microarray data using qRT-PCR and Western blot analysis for representative genes. (A) qRT-PCR analysis in comparison to the microarray data for mRNAs with altered total levels. (B) qRT-PCR analysis in comparison to the microarray data for mRNAs where translation was down-regulated on the microarrays. (C) qRT-PCR analysis in comparison to the microarray data for mRNAs where translation was up-regulated on the microarrays. (D) Western blot analysis of total protein levels from mRNAs that were translationally up-regulated following glucose starvation. (E) Western blot analysis of total protein levels from mRNAs that were translationally down-regulated following glucose starvation.

analysis was observed for mRNAs that exhibited either decreased (Figure 5B) or increased (Figure 5C) association with polysomes. Therefore good correlations between the trends observed in the microarray and qRT-PCR data were found at both the transcript and translation levels although, as has been observed previously (Cridge *et al.*, 2010), slightly more pronounced fold changes were often observed with the qRT-PCR (Figure 5, A–C).

A key question is whether the increases in mRNA level and the degree of mRNA association with polysomes cause increases in the steady-state levels of specific proteins. This question is especially important given the results described earlier in the text and in previous studies that glucose starvation causes a massive reduction in global protein synthesis. To directly assess this, Western blot analysis was performed for the selected proteins Tkl2p, Sol4p, and Sdh1p following a 30-min starvation period. The microarray data predict an increase in both the mRNA and the level of translation for *TKL2* and *SOL4*, whereas for *SDH1* only the level of translation is predicted to increase. For all three proteins, increased protein was observed relative to Rps3p, which did not significantly change in the microarrays (Figure 5D). Both *TKL2* and *SDH1* are present in the highly refined list of regulated mRNAs (Supplemental Tables S2 and S3), whereas *SOL4* is taken from the list of mRNAs before application of the *q* value cut-off and therefore likely represents a false negative. Decreases in protein abundance on the Western blots were also observed for Rna1p and Sap185p, which exhibited significantly less polysome association in the micorarrays, relative to Rps3p (Figure 5E). Overall, the alterations in both polysome association and level for specific mRNAs from the microarrays convert into defined alterations in the level of protein product. The translational up-regulation of specific mRNAs is particularly noteworthy given that under conditions of glucose starvation global protein production is repressed by >35-fold (Ashe *et al.*, 2000).

Bioinformatic analysis of translationally altered mRNAs

The highly refined list of up- and down-regulated mRNAs were next examined in more detail to ascertain whether any specific patterns emerged that might be predictive or might generate mechanistic insight. There appears to be no enrichment for mRNAs with signal peptide sequences, no significant difference in mRNA or UTR length, and no obvious sequence patterns in the 5′ and 3′ UTRs of the translationally altered mRNAs (unpublished data).

An analysis of the nucleotide content of 5′ UTR elements did reveal some differences, however, between translationally up- and down-regulated data sets. In particular, the GC content immediately upstream of the AUG start codon was lower in the up-regulated mRNAs than in the unaffected mRNAs (Figure 6A). This trend is particularly intriguing for a number of reasons. First, it has previously been suggested that A-rich sequences serve as IRES elements to promote translation initiation near the AUG start codon following glucose limitation (Gilbert *et al.*, 2007). The trend described here, where a low GC content correlates with translational activity under glucose starvation conditions, might also agree with this model. Second, the dissociation of eIF4A as a consequence of glucose starvation (described earlier) would favor initiation on mRNAs with nonstructured 5′ UTR sequences, and a lower GC content would be predicted for such mRNAs (Gu *et al.*, 2010). As shown in the model in Figure 8 later in this article, however, we cannot rule out the possibility that other ATP-dependent RNA helicases (Parsyan *et al.*, 2011), such as Ded1p, substitute for eIF4A allowing translation of these mRNAs.

Up-regulation of the pentose phosphate pathway facilitates adaptation to glucose starvation

We noted that several pentose phosphate pathway mRNAs are coordinately regulated at both the transcript and translational levels following glucose starvation (Figure 4B). Indeed, we made use of some of these in our validation analysis (e.g., Tkl2p and Sol4p; Figure 5D). Intriguingly, these mRNAs are also regulated during the response to amino acid starvation (Figure 6B; Smirnova *et al.*, 2005). To investigate whether this coordinated regulation of the pentose phosphate pathway might be important during the diauxic shift from glucose to ethanol (fermentation to respiration), yeast strains deleted for various pentose phosphate components were analyzed during a switch from glucose- to ethanol-/glycerol-containing media. On glucose media no significant difference was observed in the growth rate of the pentose phosphate deletion mutants relative to the wild-type strain, whereas on ethanol/glycerol the pentose phosphate pathway mutants exhibited a slight

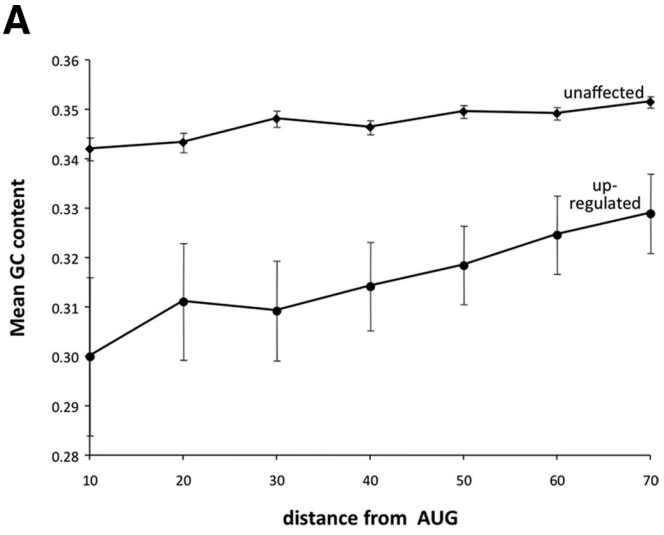

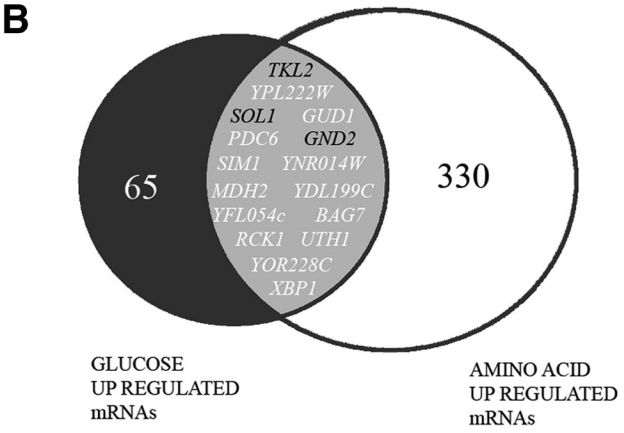

FIGURE 6: Differences in the 5′ UTR between the translationally altered gene sets and an overlap in up-regulated genes following glucose and amino acid starvation were observed. (A) Analysis of the 5′ UTR between the translationally up-regulated and unaffected data sets reveals a statistically relevant reduction in the GC content immediately upstream of the start codon among up-regulated genes compared with the rest of the mRNAs on the array. (B) Comparison of the translationally up-regulated genes from the glucose array and that of a previous study involving amino acid starvation suggest an overlap in genes up-regulated in response to these stresses, including members of the pentose phosphate pathway (highlighted).

reduction in growth rate relative to the wild-type strain (Table 1). Following a switch from glucose media to growth on the ethanol/glycerol medium under conditions that mimic the diauxic shift, a prolonged lag period that was much more protracted in the pentose phosphate pathway mutants was observed (Table 1). Polysome gradient analysis of strains switched from glucose to ethanol/glycerol medium showed the same dramatic polysome run-off that is observed following either glucose depletion (Ashe *et al.*, 2000) or glucose exhaustion from a batch culture (Figure 1). This polysome run-off is maintained during the entire lag phase caused by the switch from glucose to ethanol/glycerol media. Hence, for the pentose phosphate pathway mutants, polysome run-off is maintained for a longer period than for the wild-type strain (Figure 7). These results suggest that the pentose phosphate pathway is required for a yeast culture to adapt to a respiratory carbon source and that a coordinated transcriptional and translational up-regulation of the pentose phosphate pathway at early points in the starvation response could reflect a preemptive adaptive response required to facilitate the metabolic switch to a respiratory carbon source.

DISCUSSION

In these studies, we show that translation initiation is rapidly inhibited during glucose depletion and during the diauxic shift from glucose to ethanol growth in yeast. However, specific mRNAs are translationally maintained or activated under such conditions, and the 5′ UTR of these mRNAs is more likely to have a low GC content. Furthermore, the identification of mRNAs that are translationally resistant to glucose starvation has allowed the discovery of a cellular translation reprogramming strategy: activation of the pentose phosphate pathway in preparation for the rigors of respiratory metabolism.

The mechanism by which glucose starvation elicits the global down-regulation of translation initiation involves alterations in the protein–protein interactions within the 48S preinitiation complex. For instance, eIF4A is lost from such a complex, and surprisingly a detectable interaction is now formed between eIF3 and components of the closed loop complex, such as eIF4G and Pab1p. The simplest interpretation of these data is that the loss of eIF4A stalls progress in the initiation process leading to the accumulation of a stalled or partially formed 48S complex. Such a model, however, potentially conflicts with previous work in which we have shown that mRNAs and the associated closed loop complex components, eIF4E, eIF4G, and Pab1p, relocalize to cytoplasmic bodies after glucose starvation (Hoyle *et al.*, 2007). The missing factor that explains the discrepancy between these two observations is timing. The persistent interaction between eIF3 and the closed loop complex is observable 10 min after glucose depletion; however, by 30 min, this complex has broken down. Equally, the closed loop complex components do not enter cytoplasmic bodies until at least 25 min after glucose depletion. Thus our data suggest that glucose starvation inhibits events that lie downstream of 48S complex formation, and this stalled 48S complex decays over time to liberate the closed loop complex, which can relocalize to cytoplasmic bodies (Figure 8).

The loss of eIF4A from the eIF4G-containing preinitiation complex is particularly striking and lends support to a model in which the

		YPEG	
Strain	Doubling time on YPD	Lag period (h)	Doubling time post lag
Wild type	2.02 (±0.12)	16.3 (±0.3)	4.50 (±0.15)
*gnd2*Δ	2.39 (±0.17)	27.3 (±0.3)	5.87 (±0.64)
*tkl2*Δ	2.38 (±0.25)	29.0 (±1.0)	6.30 (±0.47)
*sol4*Δ	2.05 (±0.18)	29.0 (±1.0)	8.21 (±0.27)

TABLE 1: Growth of strains deleted for genes involved in the pentose phosphate pathway.

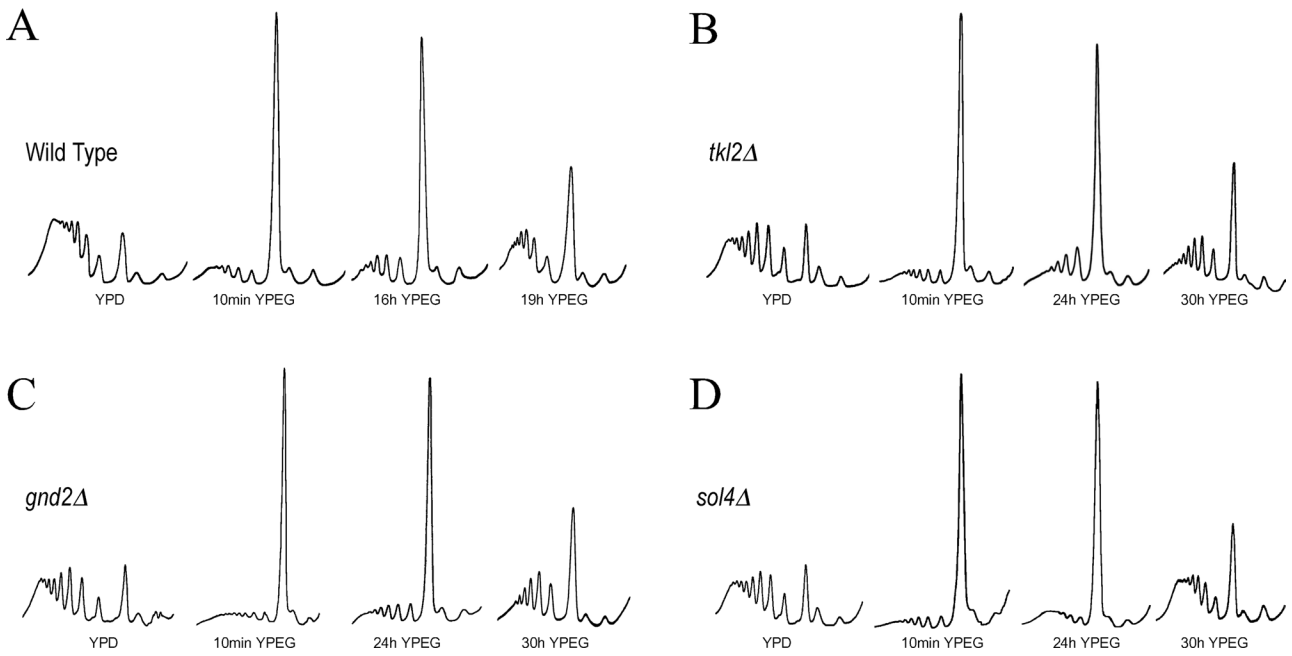

FIGURE 7: The pentose phosphate pathway is important during the diauxic shift from glucose to ethanol in *S. cerevisiae*. (A–D) Polysome profiles of *S. cerevisiae* following the switch from glucose to ethanol/glycerol media reveal a prolonged lag period, which was extended among strains deleted for different pentose phosphate pathway components.

loss of this factor ultimately explains the translational inhibition. eIF4A is thought to be one of the most abundant initiation factors across eukaryotes. For instance, estimates in yeast suggest that eIF4A is at least twofold more abundant than any other translation initiation factor and approximately fourfold more abundant than the ribosome (von der Haar and McCarthy, 2002). Therefore, in terms of translational control, eIF4A might not be perceived as a particularly attractive regulatory target within the cell. In addition, there is increasing experimental support for the idea that other RNA helicases might play important roles in translation initiation, especially where long and complex 5′ UTR structures are encountered (reviewed in Parsyan *et al.*, 2011). Therefore, as well as eIF4A being abundant, it seems plausible that redundancy may exist in its RNA unwinding functions associated with translation initiation. Nevertheless, inhibition of translation initiation via effects on eIF4A or its interactions has been identified. The effects of lithium on translation initiation in yeast are suppressed by eIF4A overexpression (Montero-Lomeli *et al.*, 2002), eIF4A functions in germ line stem cell renewal via effects on BAM (Bag-of-marbles) in the Drosophila ovary (Shen *et al.*, 2009), eIF4A is a target for the inhibitory BC1 RNA in neurons (Lin *et al.*, 2008) and a lipid signaling molecule in the anti-inflammatory response (Kim *et al.*, 2007), and, finally, the Pdcd4 tumor suppressor protein acts to inhibit translation at least partially via interaction with eIF4A (LaRonde-LeBlanc *et al.*, 2007). In addition, a variety of eIF4A targeting drugs (e.g., hippuristanol, silvestrol, and pateamine A) and eIF4A mutations have been discovered that specifically inhibit translation initiation (Blum *et al.*, 1992). It is thought that pateamine A and silvestrol act to promote the RNA binding activity of eIF4A, thus making it unavailable for interaction with the translation machinery (Bordeleau *et al.*, 2006a). In contrast, hippuristanol impairs the RNA binding, ATPase, and helicase activities of eIF4A (Bordeleau *et al.*, 2006b). Dominant-negative mutations have been characterized in which the mutant forms of

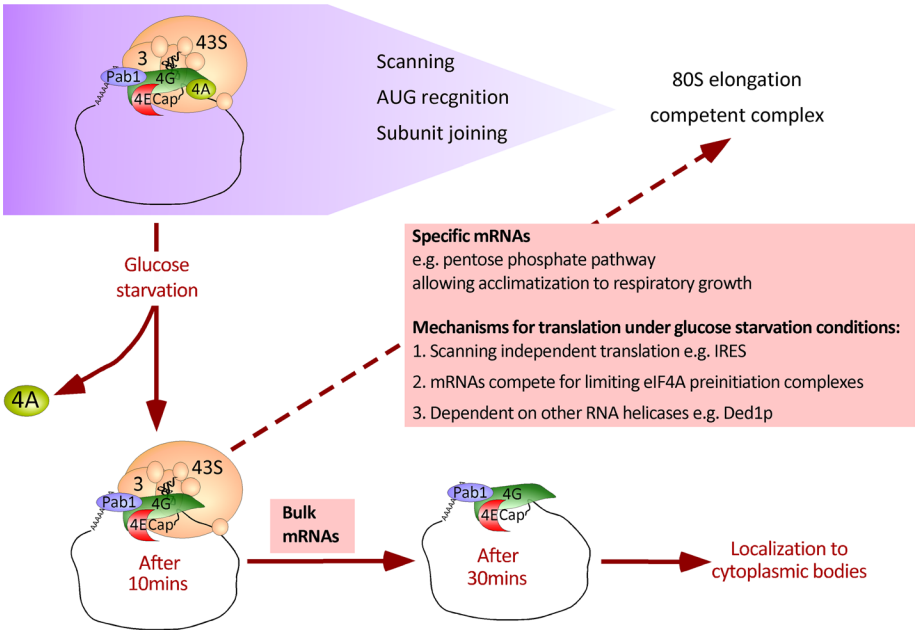

FIGURE 8: A model depicting the impact of glucose starvation on translation initiation and potential mechanisms by which specific mRNAs, such as some of those involved in the pentose phosphate pathway, may evade this regulation.

eIF4A interact with eIF4G and presumably enhance recruitment of 43S complexes but are inactive in helicase and ATPase functions (Pause *et al.*, 1994; Svitkin *et al.*, 2001). In the current study, we show that the action of glucose starvation appears to lead to eIF4A release from eIF4G, which promotes a temporary stabilization of the interaction of eIF3 with the closed loop complex. These observations suggest that eIF4A is not a requirement for the interaction of the closed loop mRNA complex with eIF3; in fact, eIF4A is required for the rapid turnover of this complex. The loss of eIF4A from the preinitiation complex is therefore a likely explanation for the rapid translational inhibition caused by glucose starvation.

An additional potential connection with the loss of eIF4A from the preinitiation complex is provided when we characterize the mRNAs that are translationally activated or maintained under glucose starvation conditions using polysome arrays. These mRNAs have a tendency to have fewer GC nucleotides in their 5′ UTRs. High GC content within RNA is well-established to favor stable RNA structures (Gu *et al.*, 2010). Therefore, the fact that low GC 5′ UTR mRNAs are translationally maintained under glucose starvation conditions may well reflect a low eIF4A requirement for their translation. Alternatively, we cannot rule out the possibility that another ATP-dependent RNA helicase(s) substitute for eIF4A on specific mRNAs.

The polysome array data also provide significant insight into the physiological consequences of glucose starvation. Starvation for glucose in yeast causes major alterations in the gene expression programs and physiology (DeRisi *et al.*, 1997). A large number of glucose repressible genes become derepressed via the combined action of the main glucose repression pathway, the Snf3/Rgt2 pathway, and the protein kinase A pathway (Rolland *et al.*, 2002). P bodies and EGP bodies, which are involved in mRNA decay and mRNA storage, are induced (Coller and Parker, 2005; Hoyle *et al.*, 2007; Buchan *et al.*, 2008). In addition, a variety of other effects of glucose starvation have been studied, including the induction of haploid invasive growth (Cullen and Sprague, 2000), dissociation of vacuolar ATPase (Dechant *et al.*, 2010), widespread relocalization of metabolic enzymes into cytoplasmic foci (Narayanaswamy *et al.*, 2009), and the rearrangement of the actin cytoskeleton (Uesono *et al.*, 2004). Connections with many of these effects can be found within our transcriptomic and polysomal array data sets.

Interrogation of the glucose starvation polysome arrays presented here clearly shows a concerted induction of the pentose phosphate pathway using both transcriptional and translational control. In terms of our glucose starvation experiments, the data from the pentose phosphate mutants suggest that induction of the pentose phosphate pathway favors cell survival on respiratory carbon sources. For instance, in the pentose phosphate pathway mutants, there is a significant increase in the length of the lag phase before growth and protein synthesis resumes following a switch from glucose to a respiratory carbon source.

The pentose phosphate pathway has a number of key functions (Wamelink *et al.*, 2008). It produces the five-carbon ribose sugar that is a precursor of a host of key molecules, including nucleotides, NAD/NADP, RNA, and DNA. In bacteria, plants, and fungi the pathway generates a starting material for the synthesis of aromatic amino acids via the Shikimate pathway. Finally, the pathway provides reducing equivalents for biosynthetic reactions and antioxidant defense pathways in the form of reduced NADP (NADPH). During a switch from fermentative to respiratory metabolism, the products of the pentose phosphate pathway could be used for a variety of purposes that would facilitate and augment this metabolic transition. For example, the NADPH could serve as reducing power for antioxidant mechanisms targeted toward the reactive oxygen species that are likely generated as a consequence of increased oxidative metabolism. In addition, the function of NADPH in a host of biosynthetic reactions (e.g., sterol biosynthesis and nucleotide production) may contribute to the well-being of cells during this metabolic transition. However, there are a variety of other sources of NADPH that compensate well for deficiencies in the pentose phosphate pathway (e.g., cytosolic NADP-specific isocitrate dehydrogenase [*IDP2*] and cytosolic NADP-specific acetaldehyde dehydrogenase [*ALD6*]) (Minard and McAlister-Henn, 2005). It is also possible that the production of ribose sugars, conceivably for the biosynthesis of nucleotides such as ATP and GTP, is the critical function of the pentose phosphate pathway during adaptation to glucose depletion. Either way, the concerted transcriptional and translational up-regulation of the pentose phosphate pathway appears to represent a preemptive induction of factors and enzymes required for an efficient transition to the respiratory program following glucose depletion in yeast.

MATERIALS AND METHODS

Strains and growth conditions

The strains used in this study are listed in Table 2. Strains were grown at 30°C on either standard yeast extract/peptone (YP) media supplemented with 2% carbon source, or synthetic complete (SC) media (Guthrie and Fink, 1991). To study the onset of respiration, the carbon source is switched to an ethanol glycerol mix (3% [vol/vol] ethanol, 1% [vol/vol] glycerol), which is well-characterized and does not support the growth of *petite* mutants (Treco and Lundblad, 2001). To switch carbon source or deplete it entirely, cells were pelleted, washed, and resuspended in the prewarmed fresh medium for various time periods. For the microarrays, cells were grown using synthetic complete glucose (SCD) medium without methionine to allow comparison to previous studies (Smirnova *et al.*, 2005). Glucose levels were determined at points in the growth on SCD media using a glucose oxidase–based glucose detection kit as described by the manufacturer (Sigma-Aldrich, St. Louis, MO). Yeast strains were C-terminally tagged with a TAP cassette using a PCR-based assay and plasmid pYM13 (Janke *et al.*, 2004). TAP-tagging was confirmed by both PCR and Western blot analysis. Standard methods were used for measuring β-galactosidase activity from strains bearing *GCN4–lacZ* fusions (Lucchini *et al.*, 1984). β-galactosidase is expressed as nanomoles of *o*-nitrophenol-β-D-galactopyranoside (ONPG) hydrolyzed per minute per microgram of total protein. The *caf20Δ eap1Δ* mutant was generated by crossing the two haploid single mutants yMK591 and yMK648 (BY background), sporulating the diploid, then dissecting tetrads. The various single- and double-mutant strains (yMK1750-3) were validated via PCR on genomic DNA samples.

TAP affinity chromatogaphy

Yeast cultures were grown to an OD_{600} of 0.6, and cells were pelleted and resuspended in YPD (yeast extract/peptone/glucose) or YP media. Cells were incubated for 10 min at 30°C and pelleted. Cell pellets were snap frozen in liquid nitrogen and ground under liquid nitrogen. Lysed cells were thawed on ice in buffer D (20 mM HEPES, pH 7.9, 50 mM KCl, 0.2 mM EDTA, 20% glycerol, 0.5 mM dithiothreitol [DTT], 0.5 mM PMSF, 1 × complete EDTA-free protease inhibitor cocktail tablet [Roche, Basel, Switzerland]). Lysates were cleared by centrifugation at 5000 rpm for 10 min at 4°C, following by 10,000 rpm for 15 min at 4°C. Protein extract (50 mg) was loaded sequentially onto 300 µl of sepharose 4B resin (GE Healthcare, Little Chalfont, Bucks., UK) prewashed with 5 ml of buffer D for 30 min at 4°C, then onto 300 µl of immunoglobulin G (IgG) sepharose 6 fast flow resin (GE Healthcare) prewashed with 5 ml of

Strain	Genotype	Source
yMK36	*MATa ade2-1 his3-11,15 leu2-3112 trp1-1 ura3-1can1-100 GCD1-S180*	Ashe *et al.*, 2001
yMK591	*MATa his3Δ1 leu2Δ0 met15Δ0 ura3Δ0 eap1::kanMX4*	Euroscarf
yMK648	*MATα his3Δ1 leu2Δ0 lys2Δ0 ura3Δ0 caf20::kanMX4*	Euroscarf
yMK926	*MATa ade-1 HIS3 leu2-3112 trp1-1 ura2-1 can1-100GCD1-P180 p[GCN4-lacZ URA3 CEN]*	Holmes *et al.*, 2004
yMK1316	*MATa ade2-1 his3-11,15 leu2-3112 trp1-1 ura3-1can1-100 GCD1-S180 TIF4631-TAP::kanMX4*	This study
yMK1338	*MATa ade2-1 his3-11,15 leu2-3112 trp1-1 ura3-1can1-100 GCD1-S180 PRT1-TAP::kanMX4*	This study
yMK1341	*MATa ade2-1 his3-11,15 leu2-3112 trp1-1 ura3-1can1-100 GCD1-P180 TIF1-TAP::kanMX4*	This study
yMK1342	*MATa ade2-1 his3-11,15 leu2-3112 trp1-1 ura3-1can1-100 GCD1-S180 PAB1-TAP::kanMX4*	This study
yMK1709	*MATa ade2 arg4 leu2-3112 trp1-289 ura3-52 TKL2-TAP::URA3*	Euroscarf
yMK1710	*MATa ade2 arg4 leu2-3112 trp1-289 ura3-52 SOL4-TAP::URA3*	Euroscarf
yMK1711	*MATa ade2 arg4 leu2-3112 trp1-289 ura3-52 SDH1-TAP::URA3*	Euroscarf
yMK1712	*MATa ade2 arg4 leu2-3112 trp1-289 ura3-52 RNA1-TAP::URA3*	Euroscarf
yMK1713	*MATa ade2 arg4 leu2-3112 trp1-289 ura3-52 SAP185-TAP::URA3*	Euroscarf
yMK1718	*MATa his3Δ1 leu2Δ0 met15Δ0 ura3Δ0 sol4::kanMX4*	Euroscarf
yMK1719	*MATa his3Δ1 leu2Δ0 lys2Δ0 ura3Δ0 tkl2::kanMX4*	Euroscarf
yMK1720	*MATa his3Δ1 leu2Δ0 met15Δ0 ura3Δ0 gnd2::kanMX4*	Euroscarf
yMK1750	*MATα his3Δ1 leu2Δ0 ura3Δ0*	This study
yMK1751	*MATα his3Δ1 leu2Δ0 ura3Δ0 caf20::kanMX4*	This study
yMK1752	*MATα his3Δ1 leu2Δ0 ura3Δ0 eap1::kanMX4*	This study
yMK1753	*MATα his3Δ1 leu2Δ0 ura3Δ0 caf20::kanMX4 eap1::kanMX4*	This study

TABLE 2: Yeast strains used in this study.

IPP150 buffer (10 mM Tris-Cl [pH 8], 1% Nonidet P-40 (NP-40), 300 mM NaCl) for 2 h at 4°C. Bound protein complexes were washed with 30 ml of IPP150 buffer followed by 10 ml of TEV cleavage buffer (10 mM Tris-Cl, pH 8, 1% NP-40, 300 mM NaCl, 0.5 mM EDTA, 1 mM DTT). Protein complexes were then cleaved from the IgG resin in 1 ml of TEV cleavage buffer containing 1 × complete EDTA-free protease inhibitor cocktail and 40 U AcTEV protease (Invitrogen, Carlsbad, CA) for 2 h at room temperature. Eluates were then incubated with 300 µl of calmodulin affinity resin (Stratagene, La Jolla, CA) prewashed with 5 ml of calmodulin binding buffer (10 mM Tris-Cl, pH 8, 1% NP-40, 300 mM NaCl, 10 mM β-mercaptoethanol, 1 mM MgAc, 1 mM imidazole, 2 mM $CaCl_2$) for 2 h at 4°C. Bound protein complexes were washed twice with calmodulin binding buffer and eluted in 1 ml of calmodulin elution buffer (10 mM Tris-Cl, pH 8, 1% NP-40, 300 mM NaCl, 10 mM β-mercaptoethanol, 1 mM MgAc, 1 mM imidazole, 2 mM EGTA, 1 × complete EDTA-free protease inhibitor cocktail). Eluted protein complexes were concentrated to 50- µl samples using Amicon Ultra-0.5-ml centrifuge filters (Millipore, Billerica, MA).

Polyribosome analysis and microarrays

Standard polyribosome analysis was performed as described previously (Taylor *et al.*, 2010) starting with 50 ml of yeast culture. For the growth analysis of a glucose grown culture, 50 ml of culture was taken at various stages during batch culture growth and chilled rapidly in 100 µg/ml cycloheximide. For the long-term switch from glucose- to ethanol-based medium, cells were grown to OD_{600} 0.6, washed, and then diluted to OD_{600} 0.2 in prewarmed ethanol glycerol medium. At various time points, 50 ml of the culture was processed for polysome analysis. Formaldehyde polysome analysis was performed as described previously (Nielsen *et al.*, 2004; Hoyle *et al.*, 2007). Individual fractions were analyzed by SDS–PAGE and Western blotting.

The polysome microarrays were performed as described previously (Smirnova *et al.*, 2005). Briefly, cycloheximide-treated chilled cultures were snap frozen in liquid nitrogen, and cells were lysed by grinding under liquid nitrogen. Lysates were cleared by centrifugation at 5000 rpm at 4°C for 1 h. One hundred A_{260} units were loaded onto 35 ml 15–50% sucrose gradients. The samples were fractionated via centrifugation at 16,900 rpm in an SW28 rotor (Beckman, High Wycombe, Bucks., UK) for 13 h. The gradients were collected using an ISCO gradient collection and fractionation system adapted for the larger 1 × 3.5 inch centrifuge tubes and fractionated into 15 × 2.2 ml aliquots. These aliquots were collected directly into 2 volumes of Trizol (Invitrogen) and stored at –80°C. Fractions 4–8 (monosomal peaks) and 11–15 (polysomal peaks) were pooled for the subsequent RNA extractions.

For the total RNA samples, 50-ml yeast cultures were grown to an OD_{600} of 0.6 and harvested by centrifugation at 5000 rpm for 5 min. Pellets were snap frozen and then lysed by grinding in liquid nitrogen. The ground powder was then resuspended in two volumes of Trizol (2 ml) and allowed to thaw on ice. Total and polysome-fractionated RNA was further processed as described previously (Smirnova *et al.*, 2005). Briefly, 1 of volume chloroform, 150 mg/ml glycogen, and sodium acetate (0.1 M, pH 4.5) were added to the Trizol-resuspended samples and mixed by vortexing. Samples were centrifuged for either 5 min at 12,000 × *g* in eppendorfs (total RNA) or 30 min at 27,000 × *g* in 50-ml polypropylene tubes (fractionated RNA). The aqueous phase was collected, 0.8 volume of isopropanol was added, and the RNA

precipitate was collected by centrifugation at either 12 000 × *g* for 10 min (total RNA) or 27,000 × *g* for 1 h (fractionated RNA). The RNA pellet was washed in 80% ethanol and resuspended in 500 µl of diethylpyrocarbonate (DEPC)-treated water. RNA samples were then precipitated again with equal volume 4 M lithium chloride buffer for 1 h at –20°C and pelleted by centrifugation at 12 000 × *g*. Pellets were washed with 80% ethanol and resuspended in 150 µl of DEPC-treated water. RNA concentration and quality were determined by using a Nanodrop 8000 spectrophotometer (Thermo Fisher Scientific, Waltham, MA) and the 2100 Bioanalyzer (Agilent Technologies, Palo Alto, CA).

Affymetrix gene chip expression microarray analysis

Microarray assays were performed using the Yeast genome 2.0 array (Affymetrix, Santa Clara, CA) according to the manufacturer's protocols. (http://www.affymetrix.com/support/technical/manuals.affx).

Approximately 10 µg of polysomal, monosomal, or total RNA was processed into biotinylated cRNA according to Affymetrix protocols. Fifteen micrograms of biotinylated cRNA targets were fragmented and hybridized to the arrays at 45°C for 16 h. The arrays were then processed using an Affymetrix fluidics station F5450 with script F5450_0003 and stained with R-phycoerythrin conjugated to streptavidin (Molecular Probes, Eugene, OR). Microarray images were acquired using the 3000 GeneChip scanner (Affymetrix) and Gene Chip Operating System (GCOS) v1.1.1. Robust Multichip Average (RMA) normalization and further analysis were carried out using the Affymetrix library of procedures (Affy version 1.5.8) in Bioconductor (version 1.5; http://www.bioconductor.org) within R (version 2.0.1; http://www.r-project.org; Gentleman *et al.*, 2004). The normalized data sets were processed by calculating the $\log_2$ intensity ratios for total transcript levels in the presence and absence of glucose. In addition, a value termed the "translation state" was calculated for every mRNA under a specific condition by calculating the ratio of $\log_2$ intensities in polysome fractions compared with those in monosome fractions. A second ratio of these values gives the change in translation state ($\text{polysome}^{\text{stress}}$/ $\text{monosome}^{\text{stress}}$: $\text{polysome}^{\text{control}}$/ $\text{monosome}^{\text{control}}$) for an individual mRNA following stress. Previously established and validated cutoff values ($\log_2$ scale) of 0.9 (for the change in translation state) and 1.0 (for the transcript level change) were applied to the data set (Smirnova *et al.*, 2005). Genes with a statistically significant change in translation state were determined with a two-factor analysis of variance model using Limma functions lmFit and eBayes (Smyth, 2004). A list of significant genes was selected with change in translation state cutoff of 0.9 and interaction $p < 0.001$ and $q < 0.1$ (false discovery rate correction using the method of QVALUE) (Storey and Tibshirani, 2003). Clustering of these genes (226 probe sets) into eight clusters was based on transcript level profiles across the data set using a k-means clustering algorithm. Clustering was performed on the means of each sample group ($\log_2$) that had been *z*-transformed (for each probe set the mean was set to 0, SD to 1). The k-means clustering was performed on the basis of similarity of profiles (Manhattan Distance) across the data set using the "Super Grouper" plugin of maxdView software (available from http://bioinf.man.ac.uk/microarray/maxd/). Each cluster generated by k-means was ranked further by hierarchical clustering. The data sets are publicly available at ArrayExpress (E-MEXP-3037 and E-MEXP-3038), and the supplemental material contains spreadsheets bearing the full $\log_2$ scale data sets (Supplemental Table 1). To facilitate comparison to the Northern analysis, the linear scale normalized intensity values were used to calculate the appropriate polysome-to-monosome ratios in Figure 4.

RT-PCR validation

RNA analysis by real-time reverse transcription qRT-PCR was carried out using the MyiQ single-color real-time PCR detection system and iQ SYBR Green Supermix (Bio-Rad, Hercules, CA). Oligonucleotide sequences were selected using the Beacon Designer 7 package (www.premierbiosoft.com) and are listed in Supplemental Table 1. Signals were quantified relative to actin mRNA control.

Western blot analysis

Protein extracts were generated from yeast cultures grown to an OD_{600} of 0.6. Cells were pelleted by centrifugation at 5000 rpm for 5 min at 30°C, snap frozen in liquid nitrogen, and ground under liquid nitrogen. Lysed cells were thawed on ice in buffer D. Lysates were cleared by centrifugation at 10,000 rpm for 15 min at 4°C. Equal concentrations of protein extracts, TAPs, or polyribosome fractions were resolved by SDS–PAGE and electroblotted onto nitrocellulose membrane. Blots were probed using the relevant primary antibody. All primary antibodies were detected with horseradish peroxidase (HRP)-conjugated rabbit secondary antibody, with the exception of the Pab1p primary antibody, which was detected using HRP-conjugated mouse secondary antibody. For identification of the TAP tagged proteins, an HRP-conjugated primary antibody to Protein A (Abcam, Cambridge, MA) was used.

ACKNOWLEDGMENTS

This work has been supported by the Leverhulme Trust (project grant F/00 120/AN), the Wellcome Trust (project grant 080349/Z/06/Z), and the Biotechnology and Biological Sciences Research Council (BBSRC; Lola grant BB/G012571/1). We thank L. Wardleworth and A. Hayes in the Faculty of Life Sciences Genomic Technologies/Bioinformatics Research Facility at the University of Manchester for providing technical support and advice with regard to Affymetrix arrays.

REFERENCES

Ashe MP, De Long SK, Sachs AB (2000). Glucose depletion rapidly inhibits translation initiation in yeast. Mol Biol Cell 11, 833–848.

Ashe MP, Slaven JW, De Long SK, Ibrahimo S, Sachs AB (2001). A novel eIF2B-dependent mechanism of translational control in yeast as a response to fusel alcohols. EMBO J 20, 6464–6474.

Blum S, Schmid SR, Pause A, Buser P, Linder P, Sonenberg N, Trachsel H (1992). ATP hydrolysis by initiation factor 4A is required for translation initiation in Saccharomyces cerevisiae. Proc Natl Acad Sci USA 89, 7664–7668.

Bordeleau ME, Cencic R, Lindqvist L, Oberer M, Northcote P, Wagner G, Pelletier J (2006a). RNA-mediated sequestration of the RNA helicase eIF4A by Pateamine A inhibits translation initiation. Chem Biol 13, 1287–1295.

Bordeleau ME, Mori A, Oberer M, Lindqvist L, Chard LS, Higa T, Belsham GJ, Wagner G, Tanaka J, Pelletier J (2006b). Functional characterization of IRESes by an inhibitor of the RNA helicase eIF4A. Nat Chem Biol 2, 213–220.

Buchan JR, Muhlrad D, Parker R (2008). P bodies promote stress granule assembly in Saccharomyces cerevisiae. J Cell Biol 183, 441–455.

Cherkasova V, Qiu HF, Hinnebusch AG (2010). Snf1 Promotes phosphorylation of the alpha subunit of eukaryotic translation initiation factor 2 by activating Gcn2 and inhibiting phosphatases Glc7 and Sit4. Mol Cell Biol 30, 2862–2873.

Coller J, Parker R (2005). General translational repression by activators of mRNA decapping. Cell 122, 875–886.

Cridge AG, Castelli LM, Smirnova JB, Selley JN, Rowe W, Hubbard SJ, McCarthy JE, Ashe MP, Grant CM, Pavitt GD (2010). Identifying eIF4E-binding protein translationally-controlled transcripts reveals links to mRNAs bound by specific PUF proteins. Nucleic Acids Res 38, 8039–8050.

Cullen PJ, Sprague GF Jr (2000). Glucose depletion causes haploid invasive growth in yeast. Proc Natl Acad Sci USA 97, 13619–13624.

Dechant R, Binda M, Lee SS, Pelet S, Winderickx J, Peter M (2010). Cytosolic pH is a second messenger for glucose and regulates the PKA pathway through V-ATPase. EMBO J 29, 2515–2526.
Deloche O, de la Cruz J, Kressler D, Doere M, Linder P (2004). A membrane transport defect leads to a rapid attenuation of translation initiation in Saccharomyces cerevisiae. Mol Cell 13, 357–366.
DeRisi JL, Iyer VR, Brown PO (1997). Exploring the metabolic and genetic control of gene expression on a genomic scale. Science 278, 680–686.
Dever TE (1997). Using GCN4 as a reporter of eIF2 alpha phosphorylation and translational regulation in yeast. Methods 11, 403–417.
Gentleman RC *et al.* (2004). Bioconductor: open software development for computational biology and bioinformatics. Genome Biol 5, R80.
Gilbert WV, Zhou K, Butler TK, Doudna JA (2007). Cap-independent translation is required for starvation-induced differentiation in yeast. Science 317, 1224–1227.
Gomez E, Powell ML, Greenman IC, Herbert TP (2004). Glucose-stimulated protein synthesis in pancreatic beta-cells parallels an increase in the availability of the translational ternary complex (eIF2-GTP center dot Met-tRNAi) and the dephosphorylation of eIF2 alpha. J Biol Chem 279, 53937–53946.
Gu W, Tong Z, Wilke CO (2010). A universal trend of reduced mRNA stability near the translation-initiation site in prokaryotes and eukaryotes. PLOS Comput Biol 6, e1000664.
Guthrie C, Fink GR (1991). Guide to Yeast Genetics and Molecular Biology, San Diego, CA: Academic Press.
He H, von der Haar T, Singh CR, Ii M, Li B, Hinnebusch AG, McCarthy JE, Asano K (2003). The yeast eukaryotic initiation factor 4G (eIF4G) HEAT domain interacts with eIF1 and eIF5 and is involved in stringent AUG selection. Mol Cell Biol 23, 5431–5445.
Hinnebusch AG (2005). Translational regulation of GCN4 and the general amino acid control of yeast. Annu Rev Microbiol 59, 407–450.
Holmes LEA, Campbell SG, De Long SK, Sachs AB, Ashe MP (2004). Loss of translational control in yeast compromised for the major mRNA decay pathway. Mol Cell Biol 24, 2998–3010.
Hoyle NP, Castelli LM, Campbell SG, Holmes LE, Ashe MP (2007). Stress-dependent relocalization of translationally primed mRNPs to cytoplasmic granules that are kinetically and spatially distinct from P-bodies. J Cell Biol 179, 65–74.
Ibrahimo S, Holmes LE, Ashe MP (2006). Regulation of translation initiation by the yeast eIF4E binding proteins is required for the pseudohyphal response. Yeast 23, 1075–1088.
Jackson RJ, Hellen CUT, Pestova TV (2010). The mechanism of eukaryotic translation initiation and principles of its regulation. Nat Rev Mol Cell Bio 11, 113–127.
Janke C *et al.* (2004). A versatile toolbox for PCR-based tagging of yeast genes: new fluorescent proteins, more markers and promoter substitution cassettes. Yeast 21, 947–962.
Kim WJ, Kim JH, Jang SK (2007). Anti-inflammatory lipid mediator 15d-PGJ2 inhibits translation through inactivation of eIF4A. EMBO J 26, 5020–5032.
Kuhn KM, DeRisi JL, Brown PO, Sarnow P (2001). Global and specific translational regulation in the genomic response of Saccharomyces cerevisiae to a rapid transfer from a fermentable to a nonfermentable carbon source. Mol Cell Biol 21, 916–927.
LaRonde-LeBlanc N, Santhanam AN, Baker AR, Wlodawer A, Colburn NH (2007). Structural basis for inhibition of translation by the tumor suppressor Pdcd4. Mol Cell Biol 27, 147–156.
LeFebvre AK, Korneeva NL, Trutschl M, Cvek U, Duzan RD, Bradley CA, Hershey JW, Rhoads RE (2006). Translation initiation factor eIF4G-1 binds to eIF3 through the eIF3e subunit. J Biol Chem 281, 22917–22932.
Lin D, Pestova TV, Hellen CU, Tiedge H (2008). Translational control by a small RNA: dendritic BC1 RNA targets the eukaryotic initiation factor 4A helicase mechanism. Mol Cell Biol 28, 3008–3019.
Lucchini G, Hinnebusch AG, Chen C, Fink GR (1984). Positive regulatory interactions of the HIS4 gene of Saccharomyces cerevisiae. Mol Cell Biol 4, 1326–1333.
Lui J, Campbell SG, Ashe MP (2010). Inhibition of translation initiation following glucose depletion in yeast facilitates a rationalization of mRNA content. Biochem Soc Trans 38, 1131–1136.
Mascarenhas C, Edwards-Ingram LC, Zeef L, Shenton D, Ashe MP, Grant CM (2008). Gcn4 is required for the response to peroxide stress in the yeast Saccharomyces cerevisiae. Mol Biol Cell 19, 2995–3007.
Melamed D, Arava Y (2007). Genome-wide analysis of mRNA polysomal profiles with spotted DNA microarrays. Methods Enzymol 431, 177–201.
Minard KI, McAlister-Henn L (2005). Sources of NADPH in yeast vary with carbon source. J Biol Chem 280, 39890–39896.
Montero-Lomeli M, Morais BLB, Figueiredo DL, Neto DCS, Martins JRP, Masuda CA (2002). The initiation factor eIF4A is involved in the response to lithium stress in Saccharomyces cerevisiae. J Biol Chem 277, 21542–21548.
Narayanaswamy R, Levy M, Tsechansky M, Stovall GM, O'Connell JD, Mirrielees J, Ellington AD, Marcotte EM (2009). Widespread reorganization of metabolic enzymes into reversible assemblies upon nutrient starvation. Proc Natl Acad Sci USA 106, 10147–10152.
Nielsen KH, Szamecz B, Valásek L, Jivotovskaya A, Shin BS, Hinnebusch AG (2004). Functions of eIF3 downstream of 48S assembly impact AUG recognition and GCN4 translational control. EMBO J 23, 1166–1177.
Palmer LK, Shoemaker JL, Baptiste BA, Wolfe D, Keil RL (2005). Inhibition of translation initiation by volatile anesthetics involves nutrient-sensitive GCN-independent and -dependent processes in yeast. Mol Biol Cell 16, 3727–3739.
Parsyan A, Svitkin Y, Shahbazian D, Gkogkas C, Lasko P, Merrick WC, Sonenberg N (2011). mRNA helicases: the tacticians of translational control. Nat Rev Mol Cell Biol 12, 235–245.
Pause A, Methot N, Svitkin Y, Merrick WC, Sonenberg N (1994). Dominant negative mutants of mammalian translation initiation factor eIF-4A define a critical role for eIF-4F in cap-dependent and cap-independent initiation of translation. EMBO J 13, 1205–1215.
Pavitt GD (2005). eIF2B, a mediator of general and gene-specific translational control. Biochem Soc Trans 33, 1487–1492.
Pestova TV, Lorsch JR, Hellen CU (2007). The mechanisms of translation initiation in eukaryotes. In: Translational Control in Biology and Medicine, ed. MB Mathews, N Sonenberg, and JWB Hershey, Cold Spring Harbor, NY: CSHL Press, 87–128.
Preiss T, Baron-Benhamou J, Ansorge W, Hentze MW (2003). Homodirectional changes in transcriptome composition and mRNA translation induced by rapamycin and heat shock. Nat Struct Biol 10, 1039–1047.
Richter JD, Sonenberg N (2005). Regulation of cap-dependent translation by eIF4E inhibitory proteins. Nature 433, 477–480.
Rolland F, Winderickx J, Thevelein JM (2002). Glucose-sensing and -signalling mechanisms in yeast. FEMS Yeast Res 2, 183–201.
Rutter J, Probst BL, McKnight SL (2002). Coordinate regulation of sugar flux and translation by PAS kinase. Cell 111, 17–28.
Scheuner D, Song B, McEwen E, Liu C, Laybutt R, Gillespie P, Saunders T, Bonner-Weir S, Kaufman RJ (2001). Translational control is required for the unfolded protein response and in vivo glucose homeostasis. Mol Cell 7, 1165–1176.
Shen R, Weng C, Yu J, Xie T (2009). eIF4A controls germline stem cell self-renewal by directly inhibiting BAM function in the Drosophila ovary. Proc Natl Acad Sci USA 106, 11623–11628.
Shenton D, Smirnova JB, Selley JN, Carroll K, Hubbard SJ, Pavitt GD, Ashe MP, Grant CM (2006). Global translational responses to oxidative stress impact upon multiple levels of protein synthesis. J Biol Chem 281, 29011–29021.
Smirnova JB, Selley JN, Sanchez-Cabo F, Carroll K, Eddy AA, McCarthy JE, Hubbard SJ, Pavitt GD, Grant CM, Ashe MP (2005). Global gene expression profiling reveals widespread yet distinctive translational responses to different eukaryotic translation initiation factor 2B-targeting stress pathways. Mol Cell Biol 25, 9340–9349.
Smyth GK (2004). Linear models and empirical Bayes methods for assessing differential expression in microarray experiments. Stat Appl Genet Mol Biol 3, Article3.
Spriggs KA, Bushell M, Willis AE (2010). Translational regulation of gene expression during conditions of cell stress. Mol Cell 40, 228–237.
Storey JD, Tibshirani R (2003). Statistical significance for genomewide studies. Proc Natl Acad Sci USA 100, 9440–9445.
Svitkin YV, Pause A, Haghighat A, Pyronnet S, Witherell G, Belsham GJ, Sonenberg N (2001). The requirement for eukaryotic initiation factor 4A (eIF4A) in translation is in direct proportion to the degree of mRNA 5′ secondary structure. RNA 7, 382–394.
Taylor EJ, Campbell SG, Griffiths CD, Reid PJ, Slaven JW, Harrison RJ, Sims PFG, Pavitt GD, Delneri D, Ashe MP (2010). Fusel alcohols regulate translation initiation by inhibiting eIF2B to reduce ternary complex in a mechanism that may involve altering the integrity and dynamics of the eIF2B body. Mol Biol Cell 21, 2202–2216.

Treco DA, Lundblad V (2001). Preparation of yeast media. Curr Protoc Mol Biol 13.1.1–13.1.7.
Uesono Y, Ashe MP, Toh-E A (2004). Simultaneous yet independent regulation of actin cytoskeletal organization and translation initiation by glucose in Saccharomyces cerevisiae. Mol Biol Cell 15, 1544–1556.
von der Haar T (2008). A quantitative estimation of the global translational activity in logarithmically growing yeast cells. BMC Syst Biol 2, 87–101.
von der Haar T, McCarthy JE (2002). Intracellular translation initiation factor levels in Saccharomyces cerevisiae and their role in cap-complex function. Mol Microbiol 46, 531–544.
Wamelink MM, Struys EA, Jakobs C (2008). The biochemistry, metabolism and inherited defects of the pentose phosphate pathway: a review. J Inherit Metab Dis 31, 703–717.
Wek RC, Jiang HY, Anthony TG (2006). Coping with stress: eIF2 kinases and translational control. Biochem Soc Trans 34, 7–11.
Wells SE, Hillner PE, Vale RD, Sachs AB (1998). Circularization of mRNA by eukaryotic translation initiation factors. Mol Cell 2, 135–140.
Yang RJ, Wek SA, Wek RC (2000). Glucose limitation induces GCN4 translation by activation of gcn2 protein kinase. Mol Cell Biol 20, 2706–2717.